Increased Myelin Content Correlates with the Longer T_2 Times of the Intra-/Extra-cellular Water in White Matter Structures

Bretta Russell-Schulz[1], Cornelia Laule[2,3], David Li[3], and Alex MacKay[1]

[1]*Physics and Astronomy, University of British Columbia, Vancouver, BC, Canada,* [2]*Pathology and Laboratory Medicine, University of British Columbia, Vancouver, BC, Canada,* [3]*Radiology, University of British Columbia, Vancouver, BC, Canada*

Introduction

The T_2 decay curve from central nervous system tissue can be separated into several exponential components. In normal brain tissue, the T_2 decay curve typically has a short T_2 component (T_2 ~ 20ms), arising from the water trapped within the myelin layers (MW); an intermediate T_2 component (T_2 ~ 80ms) from intra- and extra-cellular water (IE), and a very long T_2 component (T_2 > 2s) from cerebrospinal fluid [2]. Whittall *et al*. [2] found the ranking of white matter structures from highest to lowest MW signal fraction, and highest to lowest IE geometric mean T_2 (gmT_2), agreed (highest to lowest: posterior limb of the internal capsule, splenium of corpus callosum (CC), major forceps, genu of CC and minor forceps). In the current study the relationship between MWF and IE gmT_2 was examined in more detail. We examined a non-biological explanation for this relationship (the effects of the fitting algorithm on IE gmT_2 in the presence of increasing MWF) as well as a biological cause for the observed association (exchange between MW and IE water).

Methods

Subjects: Fourteen normal healthy subjects were examined; (mean age=27years (range=19-34); 6 males and 8 females).

MR Imaging: Imaging was conducted at 1.5T (GE Echo Speed v.5.7 software). The MR protocol consisted of a localizer, proton density (PD)-weighted and T_2-weighted images (TR=2500ms,TE:30/80ms) and a modified Carr-Purcell-Meiboom-Gill T_2 relaxation sequence (48 echoes, 5mm thick axial image acquired through the base of the genu/splenium of the corpus callosum, TR=2.12-3.8s [4,5], echo spacing = 10ms (first 32 echoes),= 50ms (last 16 echoes), 128x128 matrix, 4 averages).

Data Analysis: Regions of interest (ROIs) were drawn around different white matter structures (Figure 1). The T_2 decay curves were decomposed into an unspecified apriori number of exponentials using a non-negative least squares (NNLS) fitting algorithm (AnalyzeNNLS) [6]. The myelin water fraction (MWF) was defined as the area under the MW peak divided by the total area under the T_2 distribution for each ROI; the MW range was T_2=5ms-25ms (to exclude IE water contamination from WM structures with very broad IE peaks). The position of the IE peak was examined using the gmT_2 (mean T_2 on a logarithmic scale, T_2=25ms-600ms). The relationship between IE gmT_2 and MWF was examined by a linear regression for all structures together and each structure individually. Errors reported are the standard errors. A Students t-test determined if the slope for all structures and each individual structure was significant. The p-values for the comparison of IE gmT_2 and MWF in individual structures were Bonferroni corrected ($p < 0.00625$)), otherwise $p < 0.05$ was considered to be significant. Simulations were run to examine the effects of the NNLS fitting algorithm on IE gmT_2 and MWF. The Zimmerman and Britten [6] two-pool exchange model was fit using 'no exchange' input values of myelin water T2 (T_{2MW}) = 15ms, IE water T2 (T_{2IE}) = 117ms and MWF = 0.195.

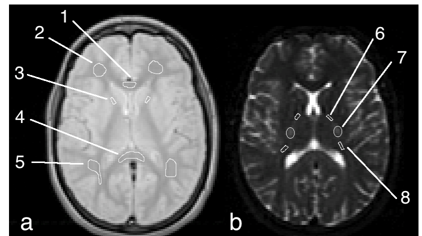

Figure 1: (a) PD image showing different ROIs 1) genu of CC, 2) minor forceps 3) AIC 4) splenium of CC and 5) major forceps. (b) Heavily T_2-weighted image TE=230ms 6) Anterior to CST 7) CST 8) Posterior to CST.

Results The IE gmT_2 and MWF showed a moderate correlation of R^2 = 0.3771 ($p = 9.61\times10^{-22}$) across all ROIs examined. Linear regressions of IE gMT_2 versus MWF for each structure individually are given in Table 1. It appears that the same relationship between IE gmT_2 and MWF does not hold for every structure. The CST and splenium of CC had the highest slopes of all structures and were the only structures that showed a significant individual relationship between IE gmT_2 and MWF. A strong correlation between average IE gmT_2 and average MWF for each structure was found, R^2 = 0.7319 ($p = 6.75\times10^{-3}$), see Figure 2. In the NNLS simulations, increasing MWF by a factor of 10 resulted in a decrease in IE gmT_2 of about 2ms, while in the experimental data the same change in MWF resulted in an increase of IE gmT_2 from 65ms to 100ms (not shown). The exchange model could be made to fit the data, see Figure 3.

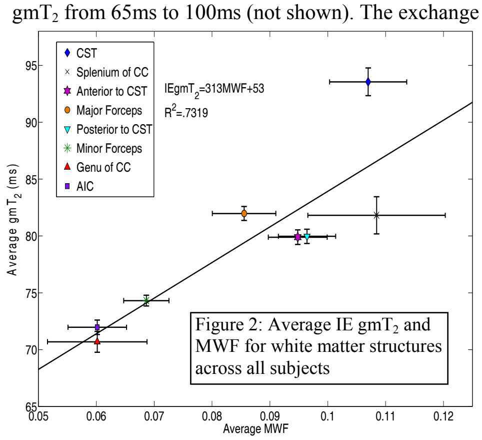

Figure 2: Average IE gmT_2 and MWF for white matter structures across all subjects

Table 1: Results of linear regression analysis between IE gmT_2 and MWF

Structure	Slope (ms)	R^2	p-value
All Structures	146 ± 13	0.3777	$\mathbf{9.61 \times 10^{-22}}$
Average	313 ± 77	0.7319	$\mathbf{6.75 \times 10^{-3}}$
CST	136 ± 77	0.5555	$\mathbf{5.35 \times 10^{-6}}$
Splenium of CC	96 ± 29	0.4835	**0.0058**
Major Forceps	65 ± 26	0.1966	0.018
Anterior to CST	42 ± 23	0.1122	0.081
Posterior to CST	47 ± 23	0.1401	0.050
Genu of CC	29 ± 28	0.0870	0.31
Minor Forceps	33 ± 23	0.0772	0.15
AIC	54 ± 22	0.1822	0.024

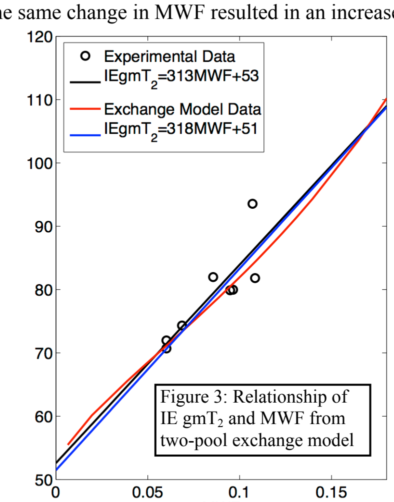

Figure 3: Relationship of IE gmT_2 and MWF from two-pool exchange model

Discussion/Conclusion

Increased MWF is accompanied by increased IE gmT_2 across white matter structures. This relationship did not appear to be the result of the NNLS fitting algorithm. The exchange model fitted our data, however the predicted T_2 times were unrealistically short (5ms). An alternative biological explanation could be increased extracellular water in structures with larger MWF; the CST is already known to have large clear spaces that could imply large amounts of extracellular water and large axons with thick sheaths [1].

References

1. Yagishita, A *et al* Radiology, 1994 2. Whittall, K.P., *et al.* Magn Reson Med, 1997 3. Sirrs, S.M., *et al.* Neuroradiology, 2007 4. Skinner MG *et al.* Magn Reson Imaging, 2007 5. Laule, C., *et al.* Magn Reson Imaging, 2007 6. Bjarnason, TA *et al.* Mag Res, 2010 7. Zimmerman, J., *et al.* J Phys Chem,1957